

PHYSICAL REVIEW B

CONDENSED MATTER AND MATERIALS PHYSICS

THIRD SERIES, VOLUME 58, NUMBER 17

1 NOVEMBER 1998-I

BRIEF REPORTS

*Brief Reports are accounts of completed research which, while meeting the usual **Physical Review B** standards of scientific quality, do not warrant regular articles. A Brief Report may be no longer than four printed pages and must be accompanied by an abstract. The same publication schedule as for regular articles is followed, and page proofs are sent to authors.*

Successive structural transitions coupled with magnetotransport properties in $\text{LaSr}_2\text{Mn}_2\text{O}_7$

T. Kimura and R. Kumai

Joint Research Center for Atom Technology (JRCAT), Tsukuba 305-0046, Japan

Y. Tokura

*Department of Applied Physics, University of Tokyo, Tokyo 113-0033, Japan
and Joint Research Center for Atom Technology (JRCAT), Tsukuba 305-0046, Japan*

J. Q. Li* and Y. Matsui

*National Institute for Research in Inorganic Materials, Tsukuba 305-0044, Japan
(Received 29 June 1998)*

Temperature variations of the lattice structure and the magnetotransport properties have been investigated for a bilayered manganite crystal $\text{LaSr}_2\text{Mn}_2\text{O}_7$ (hole-doping level of $x=0.5$) which undergoes the charge-ordering below ~ 210 K. The charge-ordered state associated with the $d_{3x^2-r^2}/d_{3y^2-r^2}$ orbital ordering of Mn^{3+} appears to collapse again with decreasing temperature below 50–100 K, which was proved by both measurements of electron and x-ray diffraction. The structural change or the switching of the orbital state in this bilayered manganite manifests itself in temperature profiles of the charge-transport and magnetic properties. [S0163-1829(98)02641-1]

The interplay of spin, charge, and lattice degrees of freedom is an issue of central importance common to many transition-metal oxides with perovskite-related structure. One of the characteristic features of these compounds is the capability of the carrier doping to an antiferromagnetic insulator by chemical substitution without disturbing the electronically active transition-metal–oxygen network. Itinerant doped carriers give rise to a variety of physical aspects such as high- T_c superconductivity and colossal magnetoresistance (MR). Doped carriers, however, often show real-space ordering and localize when the doping level (x) takes a commensurate value such as $1/2$, $1/3$, and $2/3$. Recently extensive studies^{1–5} have been performed on the $n=2$ member of the so-called Ruddlesden-Popper (RP) structure series for manganites $R_{2-2x}A_{1+2x}\text{Mn}_2\text{O}_7$ (R and A being trivalent rare-earth and divalent alkaline-earth ions, respectively) which show a wide variety of physical properties including a large MR and magnetostriction effect related to the phase transition between a paramagnetic insulator and a ferromagnetic metal. The bilayered manganite $\text{La}_{2-2x}\text{Sr}_{1+2x}\text{Mn}_2\text{O}_7$ also

shows charge-ordering behavior at a carrier concentration near $x=1/2$. Electron diffraction measurements⁶ revealed the presence of additional superlattice spots below ~ 210 K, which is the same pattern as observed for the $x=1/2, n=1$ member $\text{La}_{0.5}\text{Sr}_{1.5}\text{MnO}_4$. The observed features seem to be relevant to $d_{3x^2-r^2}/d_{3y^2-r^2}$ orbital ordering of Mn^{3+} accompanying the real-space ordering of 1:1 $\text{Mn}^{3+}/\text{Mn}^{4+}$ species.

In this paper, we report on the observation of successive structural transitions relevant to the switching of orbital state in $\text{LaSr}_2\text{Mn}_2\text{O}_7$ ($x=1/2$ in the above notation) against variation of temperature. We have observed the disappearance of the superlattice reflections at low temperatures below 50–100 K in both the electron and x-ray diffraction measurements. The results suggest that the charge-orbital ordered state appears at ~ 210 K in $\text{LaSr}_2\text{Mn}_2\text{O}_7$, but collapses at lower temperatures below 50–100 K. The structural variations dominate the temperature profiles of the charge-transport and magnetic properties.

Single crystals of $\text{LaSr}_2\text{Mn}_2\text{O}_7$ were grown by the floating zone method. We first prepared polycrystalline rods.

Powders of La_2O_3 (prior to use, dehydrated at $\sim 900^\circ\text{C}$ for ~ 12 h), SrCO_3 , and Mn_3O_4 with purities of 99.9% were weighted to the prescribed ratios, mixed, well ground, and then calcined at 1050°C for 14 hh in an alumina crucible. After regrinding, they were sintered at 1450°C for 14–30 h. The resulting powders were pulverized, and then isostatically pressed into a rod shape ($\sim 5\text{ mm}\phi \times 100\text{ mm}$) and sintered again at 1450°C for 14–30 h. The crystal growth was performed on this sintered rod with use of a halogen-lamp image furnace at a rate of 12 or 14 mm/h under an atmosphere of 1 atm O_2 . Each grown crystal was characterized by a four-circle single crystal x-ray diffractometer. The lattice parameters are $a_0 = b_0 = 3.876(4)\text{ \AA}$ and $c_0 = 20.010(4)\text{ \AA}$ with $I4/mmm$ tetragonal structure at room temperature. In this paper, to index the diffraction peaks, we will adopt the tetragonal setting. The crystal was oriented using Laue x-ray diffraction patterns, and cut into rectangular slab specimens along the main crystalline axes. Sample dimensions for the resistivity and the magnetization measurements were typically $\sim 1 \times \sim 1 \times \sim 0.2\text{ mm}^3$. Resistivity measurements were made by a conventional dc four-probe technique with current parallel (ρ_{ab}) and perpendicular (ρ_c) to MnO_2 bilayers. The electrodes on the sample were formed by heat treatment type silver paint. Magnetic fields were provided by a superconducting magnet. Magnetization measurements were performed by using a commercial dc magnetometer. We performed x-ray and electron diffraction measurements of the obtained crystals in the temperature range from room temperature to $\sim 20\text{ K}$. Measurements of electron diffraction patterns were performed by a 300 kV transmission electron microscope (Hitachi: HF-3000L), equipped with a double-tilt type of liquid helium specimen cooling holder. X-ray diffraction measurements were performed by using a low-temperature imaging plate (IP) system equipped with a closed-cycle helium refrigerator. 15° oscillation photographs for x-ray diffraction were taken for a crystal with a size of $\sim 0.2 \times \sim 0.2 \times \sim 0.1\text{ mm}^3$. Long exposure time ($\sim 120\text{ min}$) was needed to observe the weak superlattice reflections, when the x-ray generator with an Mo target (9 kW) was used.

In Fig. 1, we show the $[001]$ zone-axis electron diffraction patterns at several temperatures during (a)–(c) cooling and (d)–(f) warming runs. The diffraction pattern at 300 K [Fig. 1(a)] can be indexed with the aforementioned tetragonal unit cell. The most pronounced feature is temperature variation of the additional superstructure reflections. As presented in a previous report⁶ and also seen in Fig. 1(b), superlattice spots appear upon cooling from room temperature below $\sim 210\text{ K}$, along the $[110]$ and $[1\bar{1}0]$ directions around each fundamental Bragg reflection. The wave vector of these superlattice spots can be described as $\vec{q} = \vec{a}^*[\frac{1}{4}, \pm\frac{1}{4}, 0]$ ($\vec{a} \cdot \vec{a}^* = 1$). Figure 1(g) schematically displays the Mn^{3+} - Mn^{4+} ionic ordering and the $d_{3x^2-r^2}/d_{3y^2-r^2}$ orbital-ordering of Mn^{3+} which is consistent with the ordering wave vector of $\vec{q} = \vec{a}^*[\frac{1}{4}, \frac{1}{4}, 0]$. The two different modulations along $[110]$ and $[1\bar{1}0]$ can originate from twin domains rotated by 90° to each other. A similar pattern of the superlattice reflections has been observed for an $n=1$ single-layered manganite $\text{La}_{0.5}\text{Sr}_{1.5}\text{MnO}_4$ ($x=1/2$),^{7,8} which is attributed to orbital ordering. More recently, Murakami *et al.*⁹ performed a direct

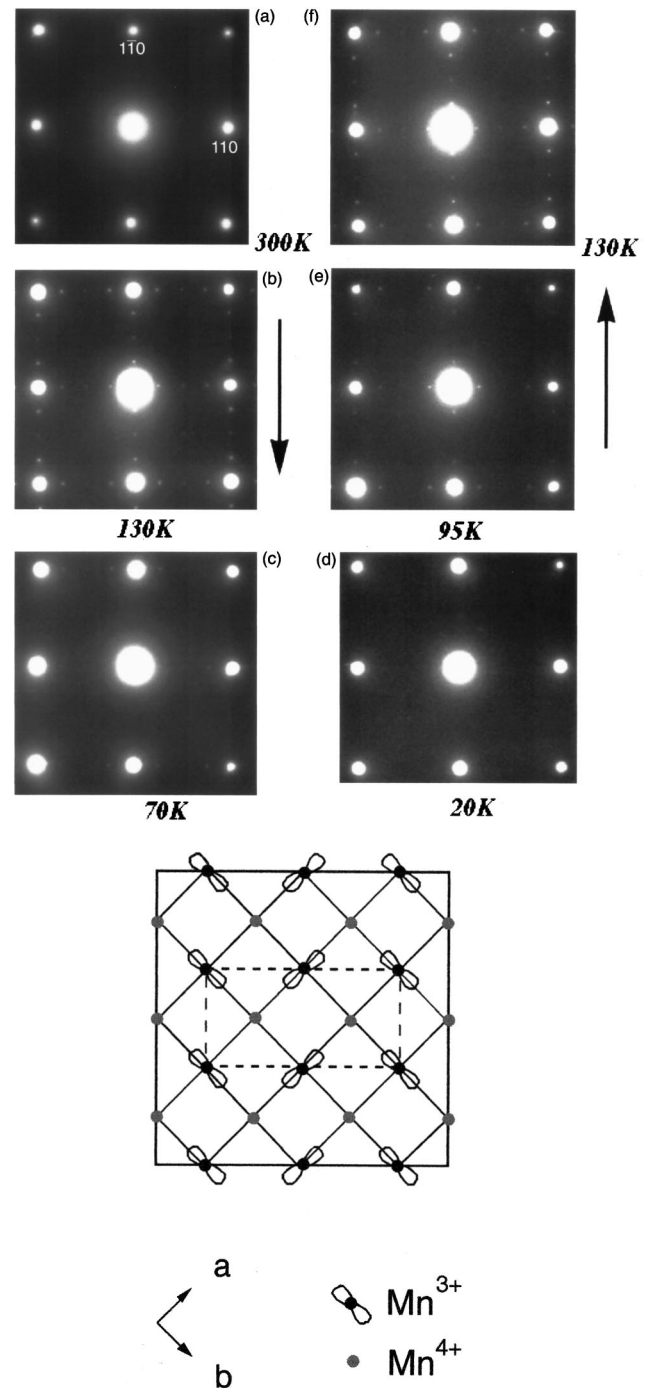


FIG. 1. $[001]$ zone-axis electron diffraction patterns of $\text{LaSr}_2\text{Mn}_2\text{O}_7$ at several temperatures during (a)–(c) cooling and (d)–(f) warming runs. The superlattice reflections show up only in the intermediate temperature region. (g) Schematic view of possible charge and orbital ordering in $\text{LaSr}_2\text{Mn}_2\text{O}_7$. Only the Mn^{3+} and Mn^{4+} ions are displayed.

x-ray observation of the orbital ordering in $\text{La}_{0.5}\text{Sr}_{1.5}\text{MnO}_4$ at a doping level of $x=1/2$ by using the anisotropy of the tensor of susceptibility (ATS) reflection technique, and revealed the concomitant charge and orbital ordering at $T_{\text{CO}} \approx 220\text{ K}$, as illustrated in Fig. 1(g). The appearance of the superlattice reflections, being identical to those in single-layered manganite, is indicative of the presence of the same pattern of the charge-orbital ordering in bilayered manganite

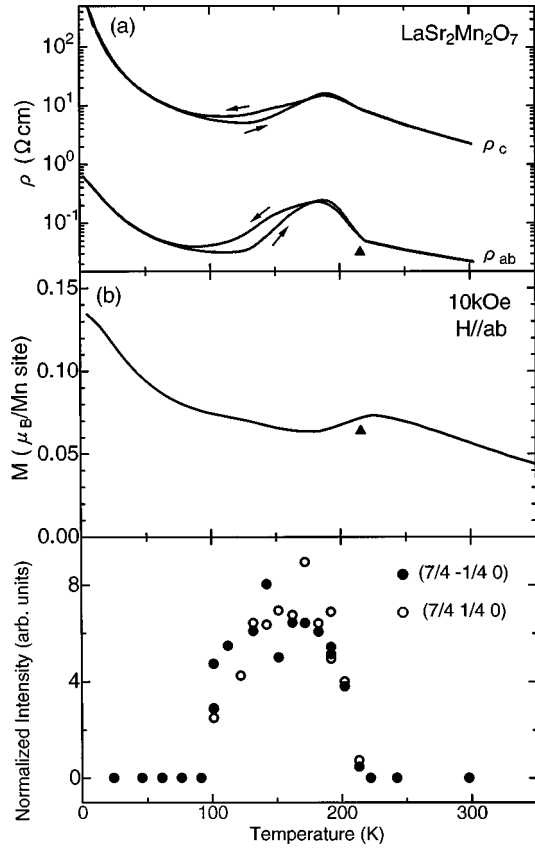


FIG. 2. Temperature dependence of (a) inplane (ρ_{ab}) and interplane (ρ_c) resistivity, (b) magnetization with $H = 10$ kOe $\parallel ab$, and (c) integrated intensity of $(\frac{7}{4}, -\frac{1}{4}, 0)$ and $(\frac{7}{4}, \frac{1}{4}, 0)$ superlattice reflection [normalized by fundamental $(2, 0, 0)$ reflection] characteristics of the orbital-ordered state, measured with an x-ray diffraction imaging plate for a $\text{LaSr}_2\text{Mn}_2\text{O}_7$ crystal. Closed triangles in (a) and (b) indicate the onset temperature of the charge ordering.

$\text{LaSr}_2\text{Mn}_2\text{O}_7$. A remarkable difference from a single-layered manganite is, however, the disappearance of the superlattice spots at low temperatures, as seen in Fig. 1(d). With increasing temperature from ~ 20 K, the superlattice reflections appear again, as displayed in Figs. 1(e) and 1(f).

Let us focus on the closely correlated features between the charge-transport and magnetic properties and structural changes in the bilayered manganite. We display in Fig. 2 the temperature profiles of (a) the resistivity, (b) the magnetization, and (c) the intensity of superlattice reflections $(\frac{7}{4}, \frac{1}{4}, 0)$ and $(\frac{7}{4}, -\frac{1}{4}, 0)$ normalized by that of the $(2, 0, 0)$ reflection which was obtained by single crystal x-ray diffraction measurements. The latter two were measured in the cooling run. The x-ray diffraction measurements confirmed the successive reentrant structural changes as well as the electron diffraction measurements: Weak superlattice reflections arising from the orbital-ordering [Fig. 1(g)] show up at $(h \pm \frac{1}{4}, k \pm \frac{1}{4}, 0)$ below ~ 210 K, as shown in Fig. 2(c). With further decreasing temperature below ~ 100 K, the superlattice spots disappear again in our experimental resolution. The results of single crystal x-ray diffraction measurements¹⁰ are thus consistent with those of electron diffraction measurements.

The resistivity was measured by cooling the sample to 4.2 K and subsequently warming them [Fig. 2(a)]. The anisotropy

ratio ρ_c/ρ_{ab} between the interplane and the inplane resistivity is $\sim 10^2$ at room temperature. Figure 2(a) shows a steep rise of ρ_{ab} toward lower temperatures around 210–220 K, where the superlattice reflections appear and the magnetization shows an anomaly [Fig. 2(b)]. With further decreasing temperature, both ρ_{ab} and ρ_c exhibit a broad peak centered at ~ 170 K, and decrease toward lower temperature in accord with the suppression of the intensity of the superlattice reflections. Another noteworthy feature in Fig. 2(a) is the presence of a remarkable hysteresis between the cooling and warming runs in the temperature region of $\sim 70 \text{ K} \leq T \leq \sim 210 \text{ K}$. Below ~ 70 K where the superlattice reflections are not observed, the thermal hysteresis also disappears, and both ρ_{ab} and ρ_c increase with decreasing temperature although the temperature dependence is much weaker than the Arrhenius-type thermal activation. The hysteretic behavior and the peak structure centered at ~ 170 K in the resistivity appears to be with charge-orbital ordering. The magnitude of ρ_{ab} ($= 10^0 - 10^1 \text{ } \Omega \text{ cm}$) in the low temperature region slightly depends on the batch, but is much lower than that in other manganites with the charge-ordered state ($\geq 10^5 \text{ } \Omega \text{ cm}$). Relatively lower values of the resistivity are also suggestive of the suppression of the charge-orbital ordered state in the low temperature region in this bilayered manganite.

Reentrant melting of the charge-ordered state with lowering temperature has been observed also in the pseudocubic manganite $\text{Pr}_{0.65}(\text{Ca}_{1-y}\text{Sr}_y)_{0.35}\text{MnO}_3$.¹¹ In this system, with decreasing temperature, the charge-ordered state appears below 200 K, but is altered to a ferromagnetic-metallic state below 100 K. The charge-orbital ordered state in $\text{Pr}_{0.65}(\text{Ca}_{1-y}\text{Sr}_y)_{0.35}\text{MnO}_3$ or related compounds can collapse into the ferromagnetic metallic state by application of magnetic fields as well. In contrast to those pseudocubic manganites, the charge-orbital ordered state in $\text{LaSr}_2\text{Mn}_2\text{O}_7$ appears to be altered to the layered antiferromagnetic (AF) state with lowering temperature, as argued in the following. Previous neutron and synchrotron x-ray powder diffraction measurements by Battle *et al.*¹² revealed that polycrystalline $\text{LaSr}_2\text{Mn}_2\text{O}_7$ synthesized by the solid state reaction separates into two phases with different carrier concentrations; $\text{La}_{1.2}\text{Sr}_{1.8}\text{Mn}_2\text{O}_7$ with ferromagnetic order below ~ 120 K and $\text{La}_{0.96}\text{Sr}_{2.04}\text{Mn}_2\text{O}_7$ with an average manganese valence of +3.52 which shows the AF order at approximately 211 K. The magnetic structure of the AF phase can be viewed as the layered antiferromagnetism in which the magnetic moments lie in the ab plane, couple ferromagnetically within the constituent single MnO_2 layer, but show AF order between the respective MnO_2 layers within a bilayer unit. These results suggest that the layered AF phase locates at carrier concentrations near $x = 0.5$. Moritomo *et al.*⁵ also proposed a phase diagram with the layered AF state around $x = 0.5$. The charge-orbital ordered state in $\text{LaSr}_2\text{Mn}_2\text{O}_7$ may be altered to such a layered AF state by decreasing the temperature. The mean field approximation for the electronic phase diagram of pseudocubic manganites predicts that the layered A-type AF state near $x = 0.5$ accompanies $d_{x^2-y^2}$ orbital ordering.¹³ If this is the case, the reentrant disappearance of the superlattice reflections may be attributed to the switching of the orbital-ordered state from staggered $d_{3x^2-r^2}/d_{3y^2-r^2}$ to uniform $d_{x^2-y^2}$.

Figure 3 displays the temperature profiles of ρ_{ab} in sev-

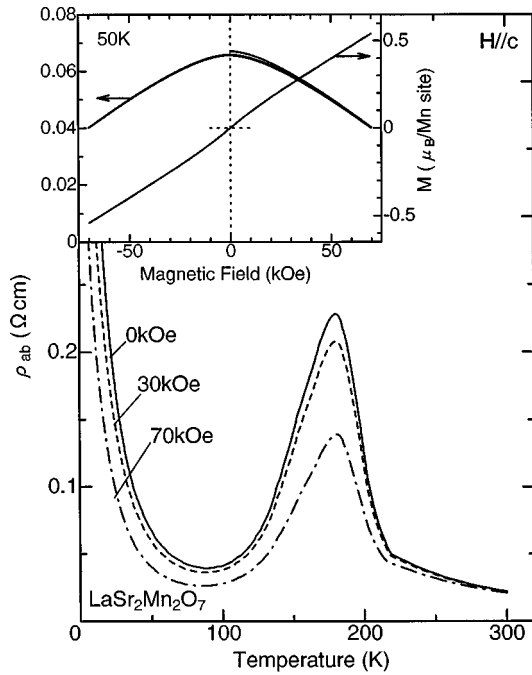


FIG. 3. Temperature dependence of ρ_{ab} in magnetic fields of 0, 30, and 70 kOe applied along the c axis in the cooling run for a $\text{LaSr}_2\text{Mn}_2\text{O}_7$ crystal. Inset: Isothermal magnetoresistance and corresponding magnetization at 50 K.

eral magnetic fields. While the magnetic field effect on ρ_{ab} is fairly small above the onset temperature of the charge-orbital ordering, a relatively large negative MR effect can be observed in the charge-orbital ordered state where ρ_{ab} is enhanced. The abrupt increase of ρ_{ab} due to the onset of charge-orbital ordering is suppressed by applying magnetic fields. Judging from the field dependence of the onset temperature of a steep increase of ρ_{ab} , the charge-orbital order-

ing transition temperature appears to decrease with increasing magnetic field ($\Delta T_{\text{CO}} \approx -3$ K at 70 kOe). Much higher fields than 70 kOe are, however, needed for the full destruction of the charge-orbital ordered state.¹⁴ In the inset of Fig. 3, we display the isothermal inplane MR and the corresponding M - H curve with $H \parallel c$ at 50 K where the charge-orbital ordering is already absent. ρ_{ab} gradually decreases in accord with the increase of the magnetization by applying magnetic fields. The nearly linear M - H curve in the layered AF state indicates that the angle of the field-induced spin canting increases at a rate of 0.13 deg/kOe. A possible origin for the low temperature MR is as follows: In the layered AF state composed of ferromagnetic single MnO_2 layers, the almost fully spin-polarized carriers are confined within the respective single MnO_2 layer and subject to the strong localization effect as observed. However, the field-induced spin-canting or ferromagnetic component may allow carrier hopping between the single layers and resultantly relax the strong localization in terms of the single-layer to bilayer crossover for the carrier dynamics.

In summary, we have investigated the close correlation among the charge-transport and magnetic properties and the structural change in the bilayered manganite crystal $\text{LaSr}_2\text{Mn}_2\text{O}_7$ (hole doping level of $x=0.5$). In this system, the charge-orbital ordered state appears below ~ 210 K. With further decreasing temperature, however, the ordered state is suppressed and finally collapses below 50–100 K. In response to the field-induced spin canting, a fairly large magnetoresistance is observed for the layered antiferromagnetic but orbital-disordered low-temperature state.

We thank Y. Tomioka, A. Asamitsu, Y. Okimoto, and T. Hayashi for helpful discussions. This work, supported in part by NEDO, was performed in JRCAT under the joint research agreement between NAIR and ATP.

*Present address: Institute of Physics, Chinese Academy of Sciences, Beijing 100080, China.

¹Y. Moritomo, A. Asamitsu, H. Kuwahara, and Y. Tokura, *Nature (London)* **380**, 141 (1996).

²T. Kimura, Y. Tomioka, H. Kuwahara, A. Asamitsu, M. Tamura, and Y. Tokura, *Science* **274**, 1698 (1996); T. Kimura, A. Asamitsu, Y. Tomioka, and Y. Tokura, *Phys. Rev. Lett.* **79**, 3720 (1997).

³J. F. Mitchell, D. N. Argyriou, J. D. Jorgensen, D. G. Hinks, K. D. Potter, and S. D. Bader, *Phys. Rev. B* **55**, 63 (1997).

⁴D. N. Argyriou, J. F. Mitchell, C. D. Potter, S. D. Bader, R. Kleb, and J. D. Jorgensen, *Phys. Rev. B* **55**, R11 965 (1997).

⁵Y. Moritomo, Y. Maruyama, T. Akimoto, and A. Nakamura, *J. Phys. Soc. Jpn.* **67**, 405 (1998).

⁶J. Q. Li, Y. Matsui, T. Kimura, and Y. Tokura, *Phys. Rev. B* **57**, R3205 (1998).

⁷Y. Moritomo, Y. Tomioka, A. Asamitsu, Y. Tokura, and Y. Matsui, *Phys. Rev. B* **51**, 3297 (1995).

⁸W. Bao, C. H. Chen, S. A. Carter, and S-W. Cheong, *Solid State Commun.* **98**, 55 (1996).

⁹Y. Murakami, H. Kawada, H. Kawata, M. Tanaka, T. Arima, Y. Moritomo, and Y. Tokura, *Phys. Rev. Lett.* **80**, 1932 (1998).

¹⁰We have also performed the same x-ray measurements of a single-layered manganite, $\text{La}_{0.5}\text{Sr}_{1.5}\text{MnO}_4$. Essentially the same patterns of superlattice reflections with the ordering wave vector of $\vec{q} = \vec{a}^*[\frac{1}{4}, \frac{1}{4}, 0]$ were observed below ~ 220 K, which persist down to the lowest temperature (~ 20 K).

¹¹Y. Tomioka, A. Asamitsu, H. Kuwahara, and Y. Tokura, *J. Phys. Soc. Jpn.* **66**, 302 (1997).

¹²P. D. Battle, D. E. Cox, M. A. Green, J. E. Millburn, L. E. Spring, P. G. Radaelli, M. J. Rosseinsky, and J. F. Vente, *Chem. Mater.* **9**, 1042 (1997).

¹³R. Maezono, S. Ishihara, and N. Nagaosa, *Phys. Rev. B* **57**, R13 993 (1998).

¹⁴T. Hayashi, N. Miura, T. Kimura, and Y. Tokura (unpublished). The rapid increase of ρ_{ab} completely disappears under the magnetic field more than ~ 200 kOe.